Acoustic Impedance Measurement through the Modelling of Ultrasonic Wave Transmission*

Ryuugo Mochizuki
Center for Socio-Robotic Synthesis, Kyushu Institute of Technology, 2-4 Hibikino Wakamatsuku Kitakyushu, 808-0196/Fukuoka, Japan†

Yuya Nishida, Kazuo Ishii
Department of Human Intelligence Systems, Kyushu Institute of Technology, 2-4 Hibikino Wakamatsuku Kitakyushu,808-0196/Fukuoka, Japan
E-mail: mochizuki.ryuugo126@mail.kyutech.jp, y-nishida@brain.kyutech.ac.jp,ishii@brain.kyutech.ac.jp
www.lsse.kyutech.ac.jp

Abstract

In food industry, shortage of workers is a serious problem. Automation of food handling is a critical nowadays. To alleviate the damage during food picking by robotic hand, we propose non-contact acoustic impedance estimation with ultrasonic wave. We have the assumption of the correlation between hardness and acoustic impedance, and, built up ultrasonic transmission model considering attenuation by reflection and absorption, then, made an experiment to estimate the impedance. As the result, we succeeded in detecting acoustic impedance without contact.

Keywords: Acoustic Impedance, Ultrasonic Transmission, Hardness, Reflection, Absorption

1. Introduction

In Japan, the demand for prepared food has been increasing recently. The survey[1] says the expenditure for prepared food has been increasing since 2004 for all human ages. The rate of the increasing expenditure is 283.9[%] for the internet shopping, 28.0[%] for convenience stores. In domestic food industry, a few millions of lunch boxes are produced and consumed a day. Food packing stage requires human resources generally[2]. For alleviation of labor burden by human, automation of food packing is effective. however, picking food by solid hand causes of damages[3]. Hardness of food should be measured without contact, then, picking force should be optimized for the automation.

We assumed relation between acoustic impedance and hardness, then estimated the impedance through analysis of ultrasonic reflection. The impedance shows the difficulty of acoustic transmission in a material, and can be estimated from reflection coefficient[4]. Confirming the relation of acoustic impedance and hardness realizes non-contact hardness measurement system.

2. Related Works

J. Machando et.al introduced ultrasonic wave into Non-Destructive Analysis for evaluation of wood strength[5].
B. Cho and J. Irudayaraj measured cheese depth with ultrasonic wave and accuracy of the measurement was 99.98[%]. Moreover, they recorded more than 0.9 of correlation between cheese mechanic property and result of sonic velocity measurement[6]. S. Srivastava et.al introduced ultrasonic measurement for hardness estimation of tomatoes, and succeeded in detecting hardness changes during the growth[7].

However, to our knowledge, no report has been found as measuring hardness unevenness. The unevenness should be considered because uniqueness of heating food is not guaranteed under cooking.

3. Proposed Method

3.1. *Outline*

Fig.1 shows the process of our acoustic impedance estimation. In the system, receiver and transmitter are attached parallel, which enables observation of reflected wave. Here, the sample is assumed as a composition of multiple media with different acoustic impedances ζ_k[Pa s/m] (k shows index of media), therefore, reflection occurs at z_k where ζ_k changes. After the transmission, we calculate amplitudes of sound pressure $P_{r,k}(z_0)$ in the reflected wave by maxima detection (Here, z_0 denotes observation point.), to easily evaluate the attenuation between reflections. Then, reflection coefficient r_k, and attenuation coefficient α_k, finally ζ_k is estimated from the result of r_k estimation. Evaluation of the correlation between ζ_k and hardness is our future work.

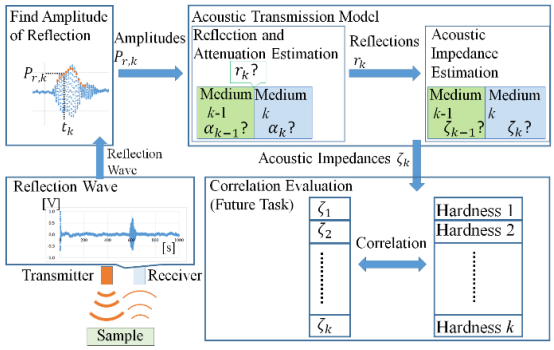

Fig. 1 Process of Acoustic Impedance Calculation

3.2. *Acoustic Transmission Model*

3.2.1. *Condition at media boundary*

In view of acoustic pressure sequence at media boundary z=z_k, the relation among incident wave (Amplitude: $P_{i,k}(z_k)$[Pa]), reflected wave (Amplitude: $P_{r,k}(z_k)$[Pa]), transmitted wave (Amplitude: $P_{t,k}(z_k)$[Pa]) is shown as Eq. (1). Here, wave frequency is ω[rad/s], sonic velocity is c_{k-1}[m/s], c_k[m/s] each other in media k-1 and k.

$$P_{i,k}(z_k)e^{j\omega\left(t-\frac{z-z_k}{c_{k-1}}\right)} + P_{r,k}(z_k)e^{j\left(t+\frac{z-z_k}{c_{k-1}}\right)} = P_{t,k}(z_k)e^{j\omega\left(t-\frac{z-z_k}{c_k}\right)}. \quad (1)$$

3.2.2. *Attenuation by Reflection*

As Fig. 2 shows, samples with uneven hardness is assumed to have multiple media of different ζ_k, thus, reflection occurs at a boundary where difference of ζ_k is observed. As Eq. (2) shows[4], small difference of ζ_k causes of the attenuation by reflection. The acoustic pressure is attenuated to r_k times of $P_{i,k}(z_k)$ after the reflection.

$$r_k = \frac{\zeta_{k-1}-\zeta_k}{\zeta_{k-1}+\zeta_k} = \frac{P_{r,k}(z_k)}{P_{i,k}(z_k)}. \quad (2)$$

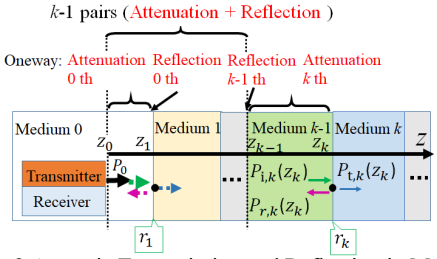

Fig. 2 Acoustic Transmission and Reflection in Media

The reflection coefficient of k-1 from k should be considered by changing the numerator of Eq. (2) into $\zeta_k - \zeta_{k-1}$. As the result, the coefficient is expressed in $-r_k$.

3.2.3. *Attenuation by Absorption*

The attenuation is caused by viscosity of media and heat transmission in the event of longitudinal wave penetration[8], whose magnitude is equal to attenuation coefficient α [Np/m][8-9]. Supposing P_0[Pa] is original acoustic pressure, and, the wave moves z [m], the pressure P diminishes as Eq. (3) shows.

$$P = P_0 e^{-\alpha z}. \quad (3)$$

We disregard wave diffusion[10] because the angle of wave expansion is enough small as our instrument.

3.2.4. *Integration of Reflection and Absorption*

As Fig. 2 shows, when P_0[Pa] is emitted at z=z_0[m] of media 0, penetration and reflection occurs at each boundary z_k. During the transmission in media k, absorption attenuation occurs in α_k[Np/m]. By the arrival at media k (z=z_k), totally, k absorptions and k-1 reflections occur. The state of incident wave (Amplitude: $P_{i,k}(z_k)$) into media k is expressed by Eq. (4).

$$P_{i,k}(z_k)e^{j\omega t} = \left\{P_0 e^{-\alpha_{k-1}(z_k - z_{k-1})} \prod_{k'=1}^{k-1} e^{-\alpha_{k'-1}(z_{k'} - z_{k'-1})}(r_{k'} + 1)\right\} e^{j\omega t} \quad (4)$$

Immediately after the reflection, the acoustic pressure of reflected wave is $P_{r,k}(z_k)$ [Pa]. By the arrival at the receiver (z=z_0), totally, k absorptions and k-1 reflections occur again. $P_{r,k}(z_k)$ is diminished to $P_{r,k}(z_0)$. This state is expressed in Eq. (5). All signs of all r_k s are opposite to Eq. (4). Eq. (4)(5) is summarized to Eq. (6)(7).

$$P_{r,k}(z_0)e^{j\omega t} = \{P_{r,k}(z_k)e^{-\alpha_{k-1}(z_k - z_{k-1})} \prod_{k'=1}^{k-1} e^{-\alpha_{k'-1}(z_{k'} - z_{k'-1})}(-r_{k'} + 1)\}e^{j\omega t}. \quad (5)$$

$$P_{r,k}(z_0)e^{j\omega t} = \{r_k P_0 e^{-2\alpha_{k-1}(z_k - z_{k-1})} \prod_{k'=1}^{k-1}(1 - r_{k'}{}^2) e^{-2\alpha_{k'-1}(z_{k'} - z_{k'-1})}\}e^{j\omega t}. \quad (6)$$

$$\frac{P_{r,k}(z_0)}{P_{r,k-1}(z_0)} = (1 - r_{k-1}{}^2)\frac{r_k}{r_{k-1}} e^{-2\alpha_{k-1}(z_k - z_{k-1})}. \quad (7)$$

3.3. *Solution*

3.3.1. *Amplitude of Reflected Wave $P_{r,k}(z_0)$*

To obtain the Amplitudes, we introduce Gradient method. From intersections with z-axis, the reflection climbs up then descends. In our condition, Large gradient (more than T_ε) should be observed at the intersections where maxima searching starts. the derivative of reflection should be T_ε or less, and the reflection should be T_p or more where candidates of $P_{r,k}(z_0)$ locate.

3.3.2. *Coefficient α_k and r_k*

Though all $P_{r,k}(z_0)$ are solved, unknown α_{k-1}, r_{k-1}, r_k are included in one equation (Eq. (7)). We introduce Monte Carlo Method to find the solutions. The relationship between α_{k-1}, r_{k-1}, r_k is expressed in Eq. (8)
From the Natural Logarithm of Eq. (7).

$$\alpha_{k-1} = \frac{1}{2(z_k - z_{k-1})} \ln\left|(1 - r_{k-1}^2)\frac{r_k}{r_{k-1}}\frac{P_{r,k-1}(z_0)}{P_{r,k}(z_0)}\right| . \quad (8)$$

Here, $\alpha_{k-1} \geq 0$ should be satisfied. α_{k-1}<0 means amplification, which leads a contradiction against attenuation. We treat only positive for r_k, then, necessary requirement of r_k is stated in Eq. (9) for $\alpha_{k-1} \geq 0$.

$$\frac{P_{r,k}(z_0)}{P_{r,k-1}(z_0)}\frac{r_{k-1}}{(1-r_{k-1}^2)} \leq r_k < 1 . \quad (9)$$

According to Eq. (9), left side of the inequality exceeds one depending on the combination of $P_{r,k}(z_0)$ and r_k. To solve the contradiction, Eq. (10) should be satisfied.

$$\frac{P_{r,k+1}(z_0)}{P_{r,k}(z_0)}\frac{r_k}{(1-r_k^2)} < 1. \quad (10)$$

As the result of Eq. (10), (11) is obtained as a solution.

$$0 < r_k < \frac{-P_{r,k+1}(z_0) + \sqrt{P_{r,k+1}(z_0)^2 + 4P_{r,k}(z_0)^2}}{2P_{r,k}(z_o)} . \quad (11)$$

r_k=0, 1 should be excluded so that antilogarithm of Eq. (8) is one or more. The upper limit in Eq. (11) is considered so as not to make contradiction for r_{k+1}. Finally, necessary requirement of r_k is defined as the overlapped range of Eq. (9) and (11).

4. Experiment

4.1. *Method*

In this experiment, we confirmed possibility of finding ζ_k through reflected wave analysis. In the environment (Fig. 3), transmitter and receiver were attached parallel. Sponges were prepared to remove echoes. The distance between transmitter and sample surface is L_{ss}[mm]. As the setting, L_{ss}=100[mm], frequency ω=800π[krad], sample width W_s = 100[mm], depth H_s=10[mm] (We selected ABS). We emitted ultrasonic wave and analyzed reflected wave by Monte Carlo Method generating random values of r_k within the range Eq. (9), (11), and obtained α_{k-1} following Eq. (8). Then we averaged r_k and α_{k-1} for the same k. Acoustic impedance ζ_0 is known to 4.1x10^2[Pa s/m][11], and, true ζ_k of ABS is 2.4x10^6[Pa s/m][12]. N_k , N_{rd} (=500) is the number of amplitudes, r_k subsets (Each subset includes r_1, r_2, .., r_{Nk-1}) each other. Because H_s is sufficiently thin, we ignored the difference of sonic velocity c in each layer. We calculated distance from z_0 to z_k by Eq. (12). t_k is the time to receive $P_{r,k}(z_0)$.

$$z_k - z_0 = \frac{1}{2}c(t_k - t_0) . \quad (12)$$

4.2. *Result and Discussion*

Fig. 4 shows the results of measurement. (a) shows $v_r(z_0)$, that is correspondent of reflected wave in voltage, where amplitude is shown in orange. (b)(c)(d) shows average of r_k, α_{k-1} ,ζ_k, each other. In Fig. 5, the same averages ((a)r_k, (b)α_{k-1} , (c)ζ_k,) are expressed in blue bar and the standard deviations are red. ζ_k = 2.5x10^6[Pa s/m] (at z_k=107.5[mm]) was the closest from the truth.

According to Fig. 5, 6, $v_r(z)$, r_k and ζ_k rose, while α_{k-1} decreased in deeper layer of the sample. From the point, r_k also naturally increases as $v_r(z)$ rises. However, α_{k-1} is particularly large near the surface. The deviation of α_{k-1} is outstanding in Fig. 5(b). We estimated r_1 and α_1 without P_o, then, the accuracy of ζ_1 cannot be guaranteed. r_k and ζ_k may change if truly observed value of P_0 is used for the solution. Eq. (2) can be transformed into Eq. (13)

$$\zeta_k = \frac{1+r_k}{1-r_k}\zeta_{k-1} \cdot \qquad (13)$$

Thus, ζ_k dramatically changes if r_k is near 1.0. Enhancing the accuracy of r_k is essential for higher accuracy of ζ_k.

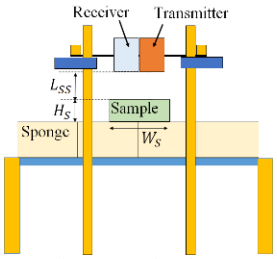

Fig. 3 Environment for the Experiment

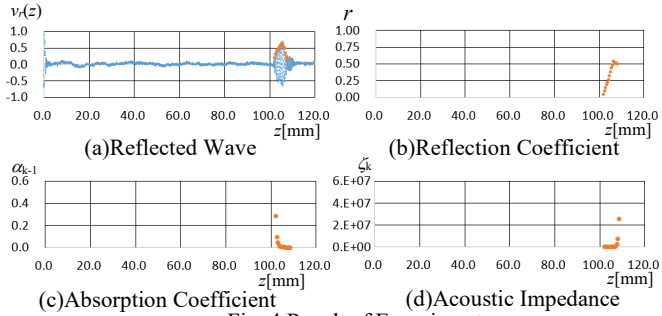

(a)Reflected Wave (b)Reflection Coefficient

(c)Absorption Coefficient (d)Acoustic Impedance

Fig. 4 Result of Experiment

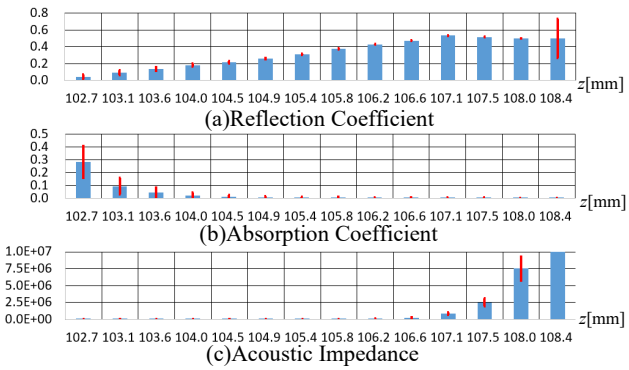

(a)Reflection Coefficient

(b)Absorption Coefficient

(c)Acoustic Impedance

Fig. 5 Averages(Blue) and Standard Deviation (Red)

5. Conclusion

In this research, we proposed acoustic impedance measurement method with ultrasonic wave. As the result, reasonable solutions of reflection coefficients were obtained in deeper layer. then accuracy of acoustic impedance estimation was 0.1[Pa s/m] error for 2.4×10^6[Pa s/m] of true ABS acoustic impedance. However, as near the surface, the solution may change according to setting of emitted acoustic pressure. Enhancing reliability in reflection coefficient estimation is necessary for better accuracy of acoustic impedance.

References

1. Yano Research Institute HP (In Japanese) https://www.yano.co.jp/press-release/show/press_id/2245
2. Ministry of Agriculture, Forestry and Fisheries, Summary of the Annual Report on Food, Agriculture and Rural Areas in Japan, MAFF, FY2017, 2017, pp. 17-18.
3. Z. Wang, M. Zhu, S. Kawamura and S. Hirai, Comparison of Different Soft Grippers for Lunch Box Packaging, *Robio*, 4:10, 2017, pp, 1-9.
4. Marine Acoustic Society of Japan, *Kaiyo Onkyo no Kiso to Oyo,* (in Japanese), *Seizando-Shoten* Publishing, 2004.
5. J. Machado, P. Palma, S. Simoes, Ultrasonic Indirect Method for Evaluating Clear Wood Strength and Stiffness, Non-Destructive Testing in Civil Engineering, 2009, pp. 1-6.
6. B. Cho and J. Irudayaraj, A Noncontact Ultrasound Approach for Mechanical Property Determination of Cheeses, *J. Food Sci.*, 68(7), 2003, pp. 2243-2247.
7. S. Srivastava, S. Vaddadi and S. Sadistap, Non-Contact Ultrasonic Based Stiffness Evaluation System for Tomatoes during Shelf-Life Storage, *Int. J. Food Sci. Nutr.*, 4(3), 2014, pp 1-6.
8. The Institute of Electronics, Information and Communication Engineers, *Chishiki* Base (In Japanese), 1(10), Chapter 2, 2014.
9. J. Carlson, J. Deventer, A. Scolan and C. Carlander, Frequency and Temperature Dependence of Acoustic Properties of Polymers Used in Pulse-Echo Systems, *Proceedings in IEEE Symposium on Ultrasonics*, 2003, pp. 885-888.
10. Y. Yokono, Measurement of Ultrasonic Attenuation in Materials, (In Japanese) Keisoku Series, Japan Welding Society, 62(7), 1993, pp. 522-527.
11. S. Takeuchi, *Hajimete no Suichu Cho-onpa* Tranceducer, (In Japanese) *J. Acoust. Soc.* of Japan, 72(5), 2016, pp. 264-272.
12. D. Serrano, A. Uris, S, Ibáñez, C. Rubio, MRI Compativle Planar Material Acoustic Lenses, *Appl. Sci.*, 8(12), 2018, pp. 1-9.

Human-Computer Communication Using Facial Expression

Yasunari Yoshitomi
Graduate School of Life and Environmental Sciences, Kyoto Prefectural University,
1-5 Nakaragi-cho, Shimogamo, Sakyo-ku, Kyoto 606-8522, Japan
E-mail: yoshitomi@kpu.ac.jp
http://www2.kpu.ac.jp/ningen/infsys/English_index.html

Abstract

To develop a complex computer system such as a robot that can communicate smoothly with humans, it is necessary to equip the system with a function for both understanding human emotions and expressing emotional signals. From both perspectives, facial expression is a promising research area. In our research, we have explored both aspects of facial expression using infrared-ray images and visible-ray images and have developed a personified agent for expressing emotional signals to humans.

Keywords: Emotion, Facial expression recognition, Infrared-ray image, Facial expression synthesis, Personified agent.

1. Introduction

The goal of our study is to present a paradigm whereby a complex computer system such as a robot can cooperate smoothly with humans. To do this, the computer system must have the ability to communicate with humans using some form(s) of information transmission. Such a system must be equipped with a function for both understanding human emotions and expressing emotional signals to its human counterparts. In this regard, facial expression is a promising target for research. Accordingly, we have been investigating both aspects of facial expression.

In this paper, we describe the challenges of reaching our goal. The remainder of the paper is organized as follows: Section 2 summarizes our studies on facial expression recognition; Section 3 briefly describes our studies on human-computer-human communication via the Internet; Section 4 outlines our studies on human-computer communication; Section 5 discusses our work on integration with speech; Section 6 concludes the paper.

2. Facial Expression Recognition

2.1. *Infrared-ray image utilization*

We have developed a method for recognizing facial expressions using thermal image processing.[1] In this study, infrared-ray was used. Figure 1 shows the influence of lighting at night on a facial image using both visible-ray ((a),(c)) and infrared-ray ((b),(d)). As is evident in the figure, the visible-ray image is strongly influenced by lighting conditions, while the thermal image is unaffected. With our method, neutral, happy, surprised, and sad facial expressions were recognized with 90% accuracy.[1] Figure 2 shows examples.

2.2. *Sensor fusion*

Sensor fusion is a promising way to improve the recognition accuracy of facial expression or emotion recognition. Several studies[2,3] to improve accuracy using sensor fusion have produced promising results.